

Daughters mimic sterile neutrinos (almost!) perfectly

Jasper Hasenkamp*

CCPP, Department of Physics, New York University, New York, NY 10003, USA

(Dated: 26th May 2014)

Since only recently, cosmological observations are sensitive to hot dark matter (HDM) admixtures with sub-eV mass, $m_{\text{hdm}}^{\text{eff}} < \text{eV}$, that are not fully-thermalised, $\Delta N_{\text{eff}} < 1$. We argue that their almost automatic interpretation as a sterile neutrino species is neither from theoretical nor practical parsimony principles preferred over HDM formed by decay products (daughters) of an out-of-equilibrium particle decay. While daughters mimic sterile neutrinos in N_{eff} and $m_{\text{hdm}}^{\text{eff}}$, there are opportunities to assess this possibility in likelihood analyses. Connecting cosmological parameters and moments of momentum distribution functions, we show that –also in the case of mass-degenerate daughters with indistinguishable main physical effects– the mimicry breaks down when the next moment, the skewness, is considered. Predicted differences of order one in the root-mean-squares of absolute momenta are too small for current sensitivities.

I. INTRODUCTION

We are in the era of precision cosmology. By observing the cosmic microwave background (CMB), the Planck satellite provided data that allows us to determine base quantities in the standard model of cosmology (Λ CDM) like the energy density of cold dark matter (CDM) on the percent level [1]. Especially, if combined with further cosmological observations, most violations of assumptions and deviations from predictions are constrained severely.

We focus on recent hints for a hot dark matter (HDM) admixture [2–4] parametrised by an effective number of additional neutrino species ΔN_{eff} and effective HDM mass of [3]

$$\Delta N_{\text{eff}} = 0.61 \pm 0.30, \quad m_{\text{hdm}}^{\text{eff}} = (0.41 \pm 0.13) \text{ eV}. \quad (1)$$

Only recently, precisions became high enough to possibly find evidence for such a *sub-eV, not fully-thermalised* species. Consequently, it is of utmost importance to scrutinise and improve the accuracy of the considered observations, see for example [5–8]. For the same reason, the time to consider such HDM admixtures independent of the exact confidence intervals is now.

The common particle physics interpretation is an additional, uncharged (= sterile) neutrino ν_s species that mixes with the active neutrinos and, consequently, is produced when these scatter in the early universe. The beauty of this interpretation is its parsimony: Firstly, there are hints from neutrino oscillation experiments for sterile neutrinos with $\mathcal{O}(\text{eV})$ masses and mixings that thermalise them. No further physics needs to be introduced, actually, from symmetry arguments one might expect even three such particles. Secondly, the cosmological model is amended by only one free parameter per particle, the sterile neutrino’s mass, since full-thermalisation fixes its temperature to the neutrino temperature and thus implies $\Delta N_{\text{eff}} = 1$. However, the cosmological sig-

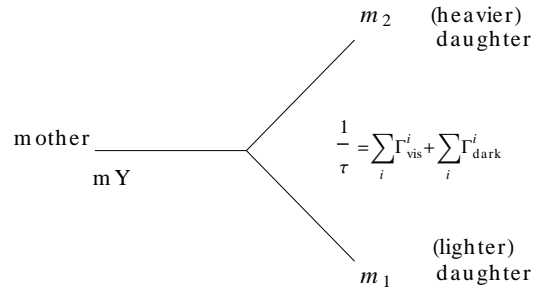


Figure 1: Our nomenclature for a cosmological particle decay and the corresponding degrees of freedom. The, in principle, arbitrarily large number is argued to reduce to three, which is further reduced to only two actually independent degrees of freedom by a physical parameter degeneracy.

nal just does not fit that interpretation as illustrated in Fig. 2.

Accepting the possibility of $\Delta N_{\text{eff}} < 1$, the cosmological model is amended by a second free parameter. Attempts to reconcile sterile neutrinos with cosmology include the addition of light, interacting particles [9] and new neutrino interactions [10, 11] that, indeed, lead to HDM improving the cosmological fit if they are gauged and shared by CDM [12]. Along the way, these ideas also give up the first parsimony argument. At that state we find it to be indicated to reconsider the interpretation of (1) being due to a thermally produced sterile neutrino (ν_s HDM), even if for the sake of identifying the limits of our understanding.

In this work, we consider the possibility that hot dark matter is formed by the decay products of an out-of-equilibrium particle decay (dpHDM). So it originates from particle decay instead of scattering. Cosmological particle decays with in part dramatic consequences are naturally expected in many theories beyond the Standard Model of particle physics (SM). They do not only occur naturally, if gravity with the prominent gravitino and Polonyi problems is considered, see [13–24] and references therein. It is remarkable that dpHDM does not require the introduction of any small mass scales as ν_s HDM.

*Electronic address: Jasper.Hasenkamp@nyu.edu

From a particle physical point of view a decay, as depicted schematically in Fig. 1, might be described by an arbitrarily large number of degrees of freedom just like a “dark sector” with new interactions. As in that case the HDM component is, nevertheless, described by only two actually independent degrees of freedom. So from an observational point of view the complexity of the cosmological models is the same.

We will explore, which scenarios of dpHDM have for what reason the potential to be distinguished from ν_s HDM and in which case dpHDM is indistinguishable from ν_s HDM in analyses like [3] utilising CMB and large-scale structure observations. In any case, the cosmological impact of dpHDM cannot be identical, because dpHDM possesses a different momentum distribution function than ν_s HDM. We will show at which point and how *any mimicry must break down*.

This work is organised as follows: In the next section we list main physical effects, define parameters and remind the case of ν_s HDM, where we also assign briefly the current observational evidence. In Sec. III we show how decay products mimic sterile neutrinos, translate observations, point out in which cases there are testable differences in the main physical effects, and how any mimicry must break down in the third cosmological parameter. In Sec. IV we summarise and conclude.

II. PRELIMINARIES

Physical effects (neutrino case) – A population of free-streaming particles, which becomes non-relativistic after photon decoupling, affects the cosmological background and the evolution of perturbations [25]. Its main physical effects are related to:

1) its contribution to the radiation energy density ρ_{rad} of the Universe before photon decoupling. Given in terms of an effective number of neutrino species N_{eff} the radiation energy density reads

$$\rho_{\text{rad}} = \left(1 + N_{\text{eff}} \frac{7}{8} \left(\frac{T_\nu}{T_\gamma}\right)^4\right) \rho_\gamma, \quad (2)$$

such that it is split into a sum of the energy density in photons $\rho_\gamma = (\pi^2/15)T^4$ and the relativistic energy density in anything else. The Standard Model of particle physics (SM) contains three active neutrinos with $N_{\text{eff}}^{\text{SM}} = 3.046$ [26] and temperature ratio $T_\nu/T_\gamma = (4/11)^{1/3}$. The small correction in $N_{\text{eff}}^{\text{SM}}$ is due to incomplete neutrino decoupling at e^+e^- -annihilation. Any departure from the standard scenario, which increases the expansion rate of the Universe and could shift the time of matter-radiation equality, is then parametrised as a summand in $N_{\text{eff}} = N_{\text{eff}}^{\text{SM}} + \Delta N_{\text{eff}}$, such that the active neutrinos correspond to $\Delta N_{\text{eff}} = 0$ by construction.

2) its non-relativistic energy density today $\rho_{\text{hdm}}^0 = n_{\text{hdm}}^0 m_{\text{hdm}}$, which is given by the mass m_{hdm} and today’s number density n_{hdm}^0 of the population. Free-

streaming particles do not cluster on scales below the free-streaming scale and thus damp fluctuations. The extent of the arising amplitude reduction in the matter power spectrum due to the free-streaming population is $\simeq 8\Omega_{\text{hdm}}/\Omega_{\text{m}}$ [25], so that the HDM fraction $f = \Omega_{\text{hdm}}/\Omega_{\text{m}}$ provides a useful parametrisation. Note that such a small HDM *admixture* leads to a step-like feature and not, for example, to a cut-off.

Assuming the active neutrinos are degenerate in mass, their today’s energy density normalised by the critical energy density ρ_c reads

$$\Omega_\nu^0 = \frac{N_{\text{eff}}^{\text{SM}} n_\gamma^0}{11 \rho_c} \sum m_\nu \Leftrightarrow \Omega_\nu^0 h^2 \simeq 0.0108 \frac{\sum m_\nu}{\text{eV}} \quad (3)$$

with today’s number density of CMB photons given by $n_\gamma^0 = (2\zeta(3)/\pi^2)T_0^3$, if $T_0 = 2.7255$ K denotes the CMB temperature today and ζ the zeta function. By construction (3) corresponds to the $\Delta N_{\text{eff}} = 0$ case. In a Λ CDM model amended to include massive (degenerate) active neutrinos this sum of neutrino masses $\sum m_\nu$ is usually “observed,” when cosmological parameters are determined. If $\sum m_\nu$ is not freed in an analysis (“pure” Λ CDM), a minimal-mass normal hierarchy can be assumed, which is accurately approximated for current cosmological data as a single massive eigenstate with $m_\nu = 0.06$ eV [1].

3) the minimum of the comoving free-streaming wavenumber k^{nr} . This is the scale at which the suppression of fluctuations in the matter power spectrum sets in. It is given by the time of the transition when the population becomes non-relativistic [25]. In Appendix A we make this point explicit arriving at

$$k^{\text{nr}} \simeq 4.08 \times 10^{-4} \Omega_{\text{m}}^{\frac{1}{2}} \left(\frac{T^{\text{nr}}}{T_0}\right)^{\frac{1}{2}} h \text{ Mpc}^{-1}, \quad (4)$$

which depends on the properties of the free-streaming population via the temperature of the Universe at transition T^{nr} only. It is defined by

$$\langle p \rangle(T^{\text{nr}}) = m, \quad (5)$$

where the angle brackets indicate the average of the particles absolute momenta, $p = |\vec{p}|$. If we kept the directional information, the population is on average at rest due to the isotropy of the Universe, $\langle \vec{p} \rangle = 0$. The root-mean-square momentum of the population equals the mean of its distribution of absolute momenta, $\langle \vec{p} \rangle_{\text{rms}} = \langle p \rangle$, which is sometimes just called “mean of the distribution“. For degenerate neutrinos (5) reads

$$\langle p_\nu \rangle(T_\nu^{\text{nr}}) = \frac{7\pi^4}{180\zeta(3)} \left(\frac{4}{11}\right)^{\frac{1}{3}} T_\nu^{\text{nr}} = \frac{1}{3} \sum m_\nu \quad (6)$$

giving

$$T_\nu^{\text{nr}} = \frac{1}{3} \left(\frac{11}{4}\right)^{\frac{1}{3}} \frac{180\zeta(3)}{7\pi^4} \sum m_\nu \simeq 0.148 \sum m_\nu. \quad (7)$$

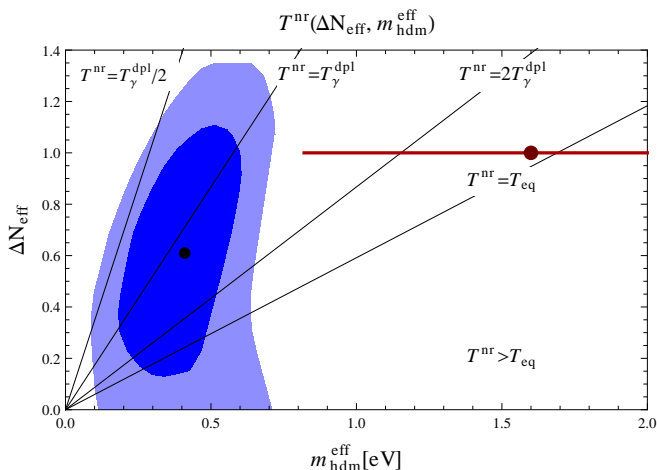


Figure 2: Joint 68%- and 95%-credible contours of the marginalised posterior found in [3] for ΔN_{eff} and $m_{\text{hdm}}^{\text{eff}}$ of a thermal sterile neutrino model with their 1-d means marked by a dot. Also marked is a best-fit value and the corresponding $3\text{-}\sigma$ range from oscillation anomalies [27] in a model with one sterile neutrino. The $1+3+1$ mass scheme with two sterile neutrinos, which actually might be preferred depending on the datasets considered, implies a large minimal mass like 3.2 eV [28].

We will use T^{nr} later on when comparing different origins of HDM. Insertion in (4) yields the expected result

$$k_{\nu}^{\text{nr}} \simeq 0.0103 \Omega_{\text{m}}^{\frac{1}{2}} \left(\frac{\sum m_{\nu}}{\text{eV}} \right)^{\frac{1}{2}} h \text{ Mpc}^{-1}. \quad (8)$$

The corresponding free-streaming scale evaluated today reads

$$\lambda_{\nu}^{\text{fs}} \simeq 24 \frac{\text{eV}}{\sum m_{\nu}} h^{-1} \text{ Mpc}. \quad (9)$$

Altogether, we see that $\sum m_{\nu}$ sets both Ω_{ν}^0 (thus f_{ν}) and T_{ν}^{nr} (thus k_{ν}^{nr}). At the same time, the neutrino temperature is fixed by SM weak interactions.

Sterile neutrino (and current evidence) – As prime example for hot thermal relics we consider a light sterile neutrino ν_s that is thermalised but with a different temperature than the active neutrinos ($\nu_s \text{HDM}$).¹ In this case the parameters under consideration are given by:

1) If T_{ν_s} denotes the temperature of the sterile neutrino population,

$$\Delta N_{\text{eff}} = \left(\frac{T_{\nu_s}}{T_{\nu}} \right)^4. \quad (10)$$

¹ In other scenarios sterile neutrinos might be produced non-thermally. As we are going to compare the decay case with thermal production, we do not include such possibilities and consider the sterile neutrino to possess a Fermi-Dirac distribution, see also Sec. III B.

Inspecting (2) we see that (10) holds by construction for a fermion. Thus a fully-thermalised neutrino species with the energy density $\rho_{1\nu} = (7/8)(4/11)^{4/3} \rho_{\gamma}$ corresponds to $\Delta N_{\text{eff}} = 1$. Other particle natures can be considered by appropriate factors in (10), for example, $4/7$ for a Nambu-Goldstone boson or $8/7$ for a massless $U(1)$ gauge boson. If the sterile neutrino shared the bath temperature once, but decoupled earlier than the active neutrinos, there is a one-to-one correspondence between its decoupling temperature $T_{\nu_s}^{\text{dpl}}$ and its temperature at later times. It is colder as it missed heating compared to the bath, when particles annihilated away. So $\Delta N_{\text{eff}} = (g_*(T_{\nu_s}^{\text{dpl}})/g_*(T_{\nu_s}^{\text{dpl}}))^{4/3}$, where g_* is the effective number of relativistic degrees of freedom and the decoupling temperature depends on the sterile neutrino's couplings to the bath.

The evidence in [3] for $\Delta N_{\text{eff}} > 0$ is mainly driven by local measurements of H_0 and seem to be supported by lensing observations [3, 4]. Independent evidence arises from the large tensor-to-scalar ratio reported by the BICEP collaboration [29]. In the simplest model of inflation a large ratio implies a large scalar spectral index that increases the power, in particular, at higher multipoles. Whereas an increased N_{eff} suppresses power at higher multipoles [30], which is due to increased Silk damping caused by the increased expansion rate [31].

2) The sterile neutrino's non-relativistic energy density today,

$$\Omega_{\nu_s}^0 = \frac{3}{11} \frac{n_{\gamma}^0}{\rho_c} \left(\frac{T_{\nu_s}}{T_{\nu}} \right)^3 \frac{m_{\nu_s}}{\text{eV}} \Leftrightarrow \Omega_{\nu_s}^0 h^2 \simeq 0.0106 \frac{m_{\text{hdm}}^{\text{eff}}}{\text{eV}}, \quad (11)$$

can be understood by comparison with (3). The case of interest is one sterile neutrino, which is much heavier than the active neutrinos. Thus the sum of neutrino masses is to be replaced by the sterile neutrino mass m_{ν_s} . The active neutrinos are then taken into account separately as a single massive eigenstate with $m_{\nu} = 0.06$ eV. Number densities decrease as $\propto T^3$, which explains the temperature ratio to the third power. We just defined the effective hot dark matter mass

$$m_{\text{hdm}}^{\text{eff}} = m_{\nu_s} (T_{\nu_s}/T_{\nu})^{1/3}. \quad (12)$$

Other particle natures can be considered by appropriate factors in (11), for example, $2/3$ for a Nambu-Goldstone boson or $4/3$ for a massive $U(1)$ gauge boson. Finally, if a hot relic decouples earlier than the active neutrinos, it does not receive any corrections from e^+e^- annihilation. Since this is the case of interest, the pre-factor is smaller by $3/N_{\text{eff}}^{\text{sm}}$. There is no factor of $1/3$, because the sterile neutrino possesses three times the mass of one degenerate neutrino in (3).

The current evidence for $m_{\text{hdm}}^{\text{eff}} > 0$ is mainly driven by galaxy cluster data [2, 3] and supported by galaxy [3, 4] as well as CMB lensing data [4]. Even before the Planck cluster count became available, cluster data has pushed evidence for $m_{\text{hdm}}^{\text{eff}} > 0$ [30, 32]. Corresponding HDM fractions f are large enough to suppress the amplitude of

matter fluctuations measured in σ_8 (= root-mean-square fluctuation in total matter in $8 h^{-1}$ Mpc spheres at $z = 0$, computed in linear theory) down to values inferred from these “local” observations. At the same time they appear small enough not to spoil the CMB fit, see also the next paragraph.

3) The average momentum of a sterile neutrino population is lowered (or increased) compared to the active neutrinos by their temperature ratio T_{ν_s}/T_ν . Comparing with (6) and (7), we find

$$T_{\nu_s}^{\text{nr}} = \frac{180\zeta(3)}{7\pi^4} \left(\frac{11}{4}\right)^{\frac{1}{3}} \frac{T_\nu}{T_{\nu_s}} m_{\nu_s} \simeq 0.445 \frac{m_{\text{hdm}}^{\text{eff}}}{\Delta N_{\text{eff}}} \quad (13)$$

Now, there is a factor of three for the reason given two paragraphs above. For completeness, we insert into (4) obtaining

$$k_{\nu_s}^{\text{nr}} \simeq 0.0178 \Omega_{\text{m}}^{\frac{1}{2}} \left(\frac{m_{\text{hdm}}^{\text{eff}}}{\text{eV}}\right)^{\frac{1}{2}} \Delta N_{\text{eff}}^{-\frac{1}{2}} h \text{ Mpc}^{-1} \quad (14)$$

and

$$\lambda_{\nu_s}^{\text{fs}} \simeq 8.1 \Omega_{\text{m}}^{\frac{1}{2}} \Delta N_{\text{eff}} \frac{\text{eV}}{m_{\text{hdm}}^{\text{eff}}} h^{-1} \text{ Mpc}. \quad (15)$$

In Fig. 2 we re-plotted the countours found in [3]. They lie roughly around the line $T_{\nu_s}^{\text{nr}} = T_\nu^{\text{dpl}}$ with an upper bound on ΔN_{eff} . If a population becomes non-relativistic before photon decoupling, $T^{\text{nr}} > T_\nu^{\text{dpl}}$, it affects the CMB directly, see e.g. [33]. The non-observation of such an impact constrains the size of $m_{\text{hdm}}^{\text{eff}}$, in particular, for large ΔN_{eff} . For smaller ΔN_{eff} the impact on the CMB decreases accordingly which allows for somewhat larger $T_{\nu_s}^{\text{nr}}$. However, the observations appear to be matched for the obtained best-fits. Even though T_ν^{nr} and $T_{\nu_s}^{\text{nr}}$ differ, there is neither preference in the data for $\sum m_\nu > 0$ with an additional source for “dark radiation” implying $\Delta N_{\text{eff}} > 0$ nor for ν_s HDM. As only difference to HDM, dark radiation is still relativistic today. For such cosmologies parameters are obtained from our work in the limit $m_{\text{hdm}}, m_1, m_2 \rightarrow 0$.

III. PERFECT(?) MIMICRY

We consider the two-body decay of a non-relativistic particle (matter or dust in the cosmological sense). We distinguish between “early” cosmological decays occurring before the onset of the BBN era, so at a time $\tau < 0.05$ s, and “late” decays occurring during or after the BBN era with $\tau > 0.05$ s. A decay during the CMB era deserves a dedicated study investigating its impact on the CMB power spectrum. Therefore, we restrict ourselves to decay times $\tau \lesssim 5.2 \times 10^{10}$ s. This is before the first observable modes of the CMB enter the horizon [34].

In principle, a decay as drawn schematically in Fig. 1 might have to be described by an arbitrarily large number of parameters: mass m and yield Y of the decaying

particle (mother) and the masses of the decay products (daughters) m_1^i, m_2^i in each existing decay mode i that sum up to the total width $\Gamma = \sum_i \Gamma_{\text{vis}}^i + \sum_i \Gamma_{\text{dark}}^i = \tau^{-1}$, where Γ_{vis}^i and Γ_{dark}^i denote partial decay widths into particles with and without electromagnetic interactions, respectively. Thus one might naively expect that there is an arbitrarily large number of possibilities for the daughters to show up in the outlined physical effects. In the following, we argue that, as far as the cosmological observables are concerned, the decay can be described by a decisively smaller number of parameters

Early decay – The case of interest is the decay of a mother that dominates the energy density of the Universe at her decay (the opposite is covered in the next subsection) and produces HDM in its decay that does not thermalise with the SM bath. The majority of the energy stored in the mother must be transferred to visible particles that unavoidably thermalise. The information how the mother decayed into visible particles – contained in all Γ_{vis}^i – is irrelevant. Instead, the following cosmology will depend on branching ratios B_i into hot dark matter B_{hdm} and SM particles B_{vis} only as they fix how the mother’s energy is distributed. We just argued $B_{\text{vis}} \simeq 1 \gg B_{\text{hdm}}$. If one allows for (additional) decay modes to produce the observed CDM, the corresponding branching ratio were restricted to be much smaller than the one into HDM, because the CDM number density needs to be much smaller. So $B_{\text{vis}} = 1 - B_{\text{hdm}}$ is either exact, if there is no additional dark decay mode, or holds to a sufficient approximation.

Concerning the kinematics, in the case of mass-degenerate daughters, $m_1 = m_2$, we define $x_2 \equiv m_2/m = m_1/m$ as measure of the mass hierarchy between mother and daughters. It might well be that the well-motivated case of daughters with similar masses, $m_1 \lesssim m_2$, is indistinguishable in cosmological observations from the case of mass-degenerate daughters. This is a subtle case that we leave for future work. If the daughters possess a large mass hierarchy, $m_1 \ll m_2$, the interesting case would be that there is a heavier daughter forming (observable) HDM and an effectively massless one not doing so and thus forming dark radiation. In that case the number of daughters forming HDM $g_{\text{hdm}} = 1$, in contrast to the mass-degenerate case with $g_{\text{hdm}} = 2$. We define $\delta \equiv (m - m_2)/m_2$ as measure of the mass hierarchy between mother and heavier daughter. Altogether, we can describe the kinematics approximately using only one hierarchy measure, x_2 or δ , depending on the case.

The mother’s energy density together with her lifetime determine the temperature of the thermal bath after her

decay T_{rh} as²

$$\rho|_{\text{dec}} = mn|_{\text{dec}} = \mu^{-1} \frac{\pi^2}{30} g_*^{\text{rh}} B_{\text{vis}}^{-1} T_{\text{rh}}^4, \quad (16)$$

where the correction factor $\mu = \mu_{\text{dom}} \simeq 0.877$ considers the exponential decay law in the expanding Universe. We determined it by solving corresponding Boltzmann equations numerically in the limit of strong dominance, $\rho \gg \rho_{\text{rad}}$, cf. [35]. Superscripts at g_* –or, if the entropy density s is considered, g_{*s} – always indicated the temperature at which the functions are evaluated.

From an, in principle, arbitrarily large number of degrees of freedom we are down to four: T_{rh} , B_{vis} (or B_{hdm}), x_2 or δ and potentially m . For an early decay the cosmological parameters under consideration are given by:

1) The relativistic HDM energy density $\rho_{\text{hdm}}|_{\text{rel}} = n_{\text{hdm}}\langle p \rangle \simeq n_{\text{hdm}}(\mu/2)m$, where it has been exploited that the daughters must be much lighter than the mother due to structure formation constraints [15]. With $n_{\text{hdm}} = g_{\text{hdm}}n$ it can be written as $\rho_{\text{hdm}}|_{\text{rel}} = \mu_{\text{dom}}\rho|_{\text{dec}}B_{\text{hdm}}(g_{\text{hdm}}/2)(T/T_{\text{rh}})^4(g_{*s}^0/g_{*s}^{\text{rh}})^{4/3}$. Inserting (16) we see that

$$\Delta N_{\text{eff}} = \frac{\rho_{\text{hdm}}|_{\text{rel}}}{\rho_{1\nu}} \simeq 8.67 \frac{B_{\text{hdm}}}{B_{\text{vis}}} \left(\frac{g_{*s}^0}{g_{*s}^{\text{rh}}} \right)^{\frac{1}{3}}. \quad (17)$$

2) Its today's (non-relativistic) energy density $\rho_{\text{hdm}}^0 = n_{\text{hdm}}^0 m_{\text{hdm}}$ can be written as $\rho_{\text{hdm}}^0 = \rho|_{\text{dec}} x_2 g_{\text{hdm}} B_{\text{hdm}} (T_0/T_{\text{rh}})^3 (g_{*s}^0/g_{*s}^{\text{rh}})$. Inserting (16) we see that it reads

$$\Omega_{\text{ed}}^0 h^2 = \frac{\rho_{\text{hdm}}^0 h^2}{\rho_c} \simeq 4.15 \mu_{\text{dom}}^{-1} \frac{x_2}{10^{-8}} \frac{B_{\text{hdm}}}{B_{\text{vis}}} \frac{T_{\text{rh}}}{\text{GeV}}. \quad (18)$$

3) The temperature of the Universe when the population of free-streaming daughters becomes non-relativistic is found as

$$\begin{aligned} T_{\text{ed}}^{\text{nr}} &= T_{\text{rh}} \frac{2}{\mu} \frac{\delta + 1}{(\delta + 1)^2 - 1} \left(\frac{g_{*s}^{\text{rh}}}{g_{*s}^0} \right)^{\frac{1}{3}} \\ \text{or} &= T_{\text{rh}} \frac{2}{\mu} (x_2^{-2} - 4)^{-\frac{1}{2}} \left(\frac{g_{*s}^{\text{rh}}}{g_{*s}^0} \right)^{\frac{1}{3}}, \end{aligned} \quad (19)$$

see (8) and (50) of [15], while $\mu = \mu_{\text{dom}}$, here. In all cases $T_{\text{dec}}^{\text{nr}} < T_{\text{eq}}$ and the minimal comoving free-streaming wavenumber of the daughters is set by (4) with T^{nr} given by (19).

² We define this temperature as the temperature of the standard thermal bath at the time of decay $T(\tau)|_{\text{rad-dom}}$ calculated in radiation domination. This temperature is known as ‘‘reheating’’ temperature, therefore, the subscript. However, the Universe is not re-heated as at the end of inflation. It just cools more slowly during the decay period. From this point of view, the notation used in the next subsection, T_d , might be seen as appropriate for this case, too. Anyway, to prevent confusion we distinguish the two cases explicitly also in the notation.

By inspection of (17) and (18) we see that the mother's mass does not enter independently. Furthermore, the observables depend on the ratio of the branching ratios $B_{\text{hdm}}/B_{\text{vis}}$ only. In other words, they depend on the amount of HDM relative to the amount of visible matter at the decay. This reduces the number of degrees of freedom in the description of the early decay to three: T_{rh} , $B_{\text{hdm}}/B_{\text{vis}}$ and a hierarchy measure, either δ or x , depending on the case under investigation.

A dominating mother produces significant entropy that dilutes relic densities during her decay. The corresponding dilution factor Δ can be given as [36]

$$\Delta = \frac{\langle g_*^{\frac{1}{3}} \rangle^{\frac{3}{4}} mY}{(g_*^{\text{rh}})^{\frac{1}{4}} T_{\text{rh}}}, \quad (20)$$

where the angle brackets indicate the appropriately-averaged value of g_* over the decay interval. We see that Δ is independent of the HDM observables. The dilution is an *additional, independent* physical effect. After discovering the primordial gravitational wave background in the CMB, we *know* that this impact of the decay will be ultimately tested by a local detection of this background radiation [37] that would rule out any such early period of matter domination.

Late decay – For $\tau > 0.05$ s current constraints on ΔN_{eff} forbid the particle to dominate the energy density of the Universe prior its decay, see Sec. 2.1 of [15].³ For such late decays, if the mother is sufficiently heavier than the proton, the branching ratio into any visible particles is constrained from BBN and CMB observations to be much smaller than one, $\sum_i \Gamma_{\text{vis}}^i \ll \sum_i \Gamma_{\text{dark}}^i$, see Sec. 3 of [15]. This holds even if photons and electrons are emitted at the end of a decay chain only, cp. [38]. If one allows for (additional) decay modes to produce the observed dark matter, the corresponding branching ratio were restricted to be much smaller than the one into hot dark matter, $\sum_i \Gamma_{\text{dark}}^i \simeq \Gamma_{\text{hdm}}$, see Sec. 4.2 of [15]. In other words, the HDM branching ratio is to a very good approximation one and the lifetime of the mother is given by her HDM decay width. This implies a decisive reduction of parameters. From an, in principle, arbitrarily large number we are down to four: mass m , yield Y and lifetime τ of the mother and one of the two hierarchy measures, δ or x_2 .

For the late decay following [15] the cosmological parameters under consideration are given by:

- 1) If $T_d = T(\tau)$ denotes the temperature of the Uni-

³ Of course, the following considerations hold for any earlier decay of a non-relativistic particle that does not dominate at its decay. There is just no observational reason that would forbid its domination.

verse at decay⁴,

$$\Delta N_{\text{eff}} = 10.25 \frac{mY}{T_d} \left(\frac{g_{*s}^0}{g_{*s}^d} \right)^{\frac{1}{3}} \frac{(\delta + 1)^2 - 1}{(\delta + 1)^2}. \quad (21)$$

Again taking into account the huge mass hierarchy, $\delta \gg 1$, required from structure formation constraints, the last fraction is also in this case to a good approximation one. This holds analogously, if the daughters are mass degenerate, see (20) of [15].

2) The non-relativistic energy density of the daughters today is given by, cf. (45) and (55) of [15],

$$\begin{aligned} \Omega_{\text{ld}}^0 &= g_{\text{hdm}} \frac{mY}{\delta + 1} \frac{g_{*s}^d}{g_{*s}^0} \frac{s_0}{\rho_c} \\ \Leftrightarrow \Omega_{\text{ld}}^0 h^2 &= \frac{2.76 \times 10^8}{\delta + 1} \frac{mY}{\text{GeV}} g_{\text{hdm}} \frac{g_{*s}^d}{g_{*s}^0}. \end{aligned} \quad (22)$$

For a decay into mass-degenerate daughters we should replace $1/(\delta + 1) \rightarrow x_2$. Note that the yield Y is the one in (21). So it is to be evaluated at the mother's decay. Into two identical particles we should replace $1/(\delta + 1) \rightarrow 2x_2 = 2m_2/m$. Note that by construction the same decay leads to both, $\Delta N_{\text{eff}} > 0$ and $m_{\text{hdm}}^{\text{eff}} > 0$. We discuss the implications of a second decay mode into dark radiation or HDM below.

3) The temperature of the Universe when the population of free-streaming daughters becomes non-relativistic is given by (19) with $\mu = \sqrt{\pi}/2$.

We inspect (21) and (22) to complete our counting of degrees of freedom in the description of a late cosmological particle decay, for the moment. We see that both observables depend on the product mY only and not on m or Y independently. They depend on the energy density at decay and not on how the energy density is built from a large mass or number density, as for an early decay. Thus observations are not sensitive to this degeneracy in determining the energy density of the mother. So instead of an arbitrarily large number of degrees of freedom we identify three: the lifetime τ , the energy density of the decaying particle $\rho (= mYs)$ and a hierarchy measure, either δ or x , depending on the case under investigation.

Even though the descriptions for the early and late decay are qualitatively different, we find in both cases three degrees of freedom that are possibly affecting the outlined three main physical effects of a free-streaming population. One might compare this to ν_s HDM with two parameters, i.e., T_{ν_s} and m_{ν_s} . In contrast to ν_s HDM, no (possibly unnatural) small mass scale needs to be introduced.

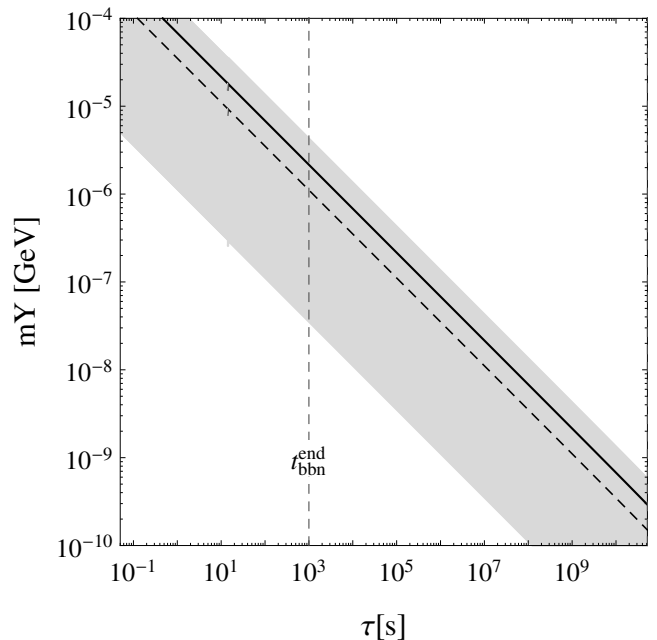


Figure 3: Determination of $mY(\tau)$ depending on T_{ν_s} exploiting (21). A higher T_{ν_s} is mimicked by a correspondingly larger energy density of the decaying particle at decay. The solid line corresponds to $N_{\text{eff}} = 0.61 \pm 0.60$ with its 2- σ range as grey band. The dashed line marks Planck's CMB only mean $\Delta N_{\text{eff}} = 0.29$ [1].

A. Translating observations

In the following we show actually that dpHDM and ν_s HDM are in general indistinguishable in CMB and large-scale structure observations using N_{eff} and $m_{\text{hdm}}^{\text{eff}}$ only. First, we provide the prescription how to obtain (for any “observed” sterile neutrino parameter) the corresponding parameters describing the cosmological particle decay with exactly the same signal. In other words, parameters determined assuming a sterile neutrino cosmology can be translated back and forth into parameters describing a cosmology with HDM originating from a cosmological particle decay.

Early decay – Comparing (10) and (17) we see trivially that a higher sterile neutrino temperature is mimicked by a larger $B_{\text{hdm}}/B_{\text{vis}}$ (for fix g_*^{rh}). Furthermore, equating (11) and (18) we find how the effective ν_s HDM mass is mimicked,

$$m_{\text{hdm}}^{\text{eff}} = \mu_{\text{dom}}^{-1} \frac{11\pi^4 g_{*s}^0}{90\zeta(3)} \frac{B_{\text{hdm}}}{B_{\text{vis}}} x_2 T_{\text{rh}}. \quad (23)$$

So the prescription is: i) Fix $B_{\text{hdm}}/B_{\text{vis}}$ to obtain the desired ΔN_{eff} . ii) Determine $x_2 T_{\text{rh}}$, while ΔN_{eff} is kept fix. At this point keep in mind that the description is valid for $T_{\text{rh}} > \text{MeV}$ only. For illustration, we translate (1)

⁴ The Universe is radiation dominated in the time window under consideration.

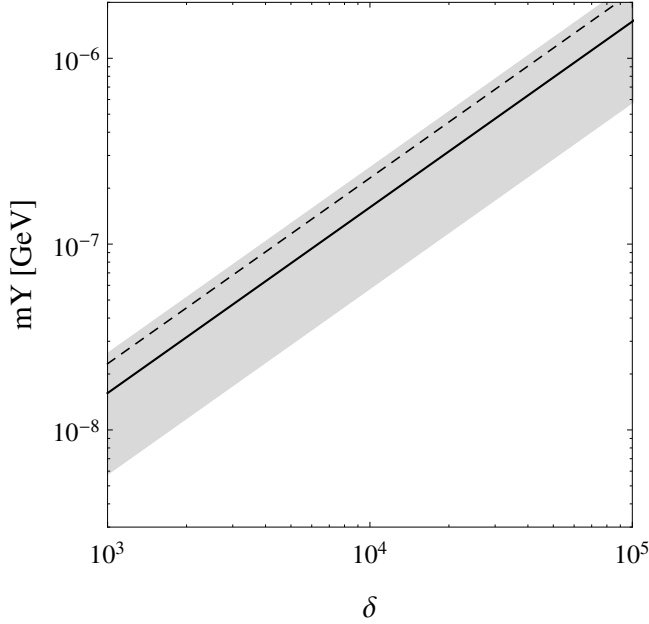


Figure 4: Determination of $mY(\delta)$ depending only on $m_{\text{hdm}}^{\text{eff}}$. A larger $m_{\text{hdm}}^{\text{eff}}$ is mimicked by a correspondingly smaller mass hierarchy. The solid line corresponds to $m_{\text{hdm}}^{\text{eff}}/\text{eV} = 0.41 \pm 0.26$ with its $2\text{-}\sigma$ range as grey band. The dashed line marks Planck’s CMB-only upper bound $m_{\text{hdm}}^{\text{eff}} < 0.59 \text{ eV}$ (95%) [1]. We have chosen $g_{\text{hdm}} = 1$ for the figure. If the decay is into mass-degenerate daughters, the horizontal axis should carry x_2^{-1} and all lines shift down by $1/2$ as $g_{\text{hdm}} = 2$.

into

$$\frac{B_{\text{hdm}}}{B_{\text{vis}}} (g_*^{\text{rh}})^{-\frac{1}{3}} = 0.045 \pm 0.022 \text{ (“1-}\sigma\text{”}; \tau < 0.05 \text{ s}) \quad (24)$$

and

$$\frac{B_{\text{hdm}}}{B_{\text{vis}}} \frac{x_2}{10^{-9} \text{ GeV}} = (9.2 \pm 2.9) \times 10^{-3} \text{ (“1-}\sigma\text{”}; \tau < 0.05 \text{ s}) \quad (25)$$

for a scenario with mass-degenerate daughters. If the daughters possess a large mass hierarchy, such that $g_{\text{hdm}} = 1$, a) nothing changes for ΔN_{eff} and b) $x_2 \rightarrow 1/(\delta + 1)$ in (25) and its right-hand-side is to be divided by 2. However, in this case there is a shift in T^{nr} as shown below and thus a difference in the main physical effects.

We would like to point out that (24) and (25) (later also (28) and (29)) are by way of illustration only. We simply “translated” parameters, while the confidence intervals are not determined by a likelihood ratio, but by the area below the posterior function that is not invariant under non-linear parameter transformations. In Sec. III B we identify (two, independent) parameters that should be determined in a Markov Chain Monte Carlo likelihood analysis with appropriate priors.

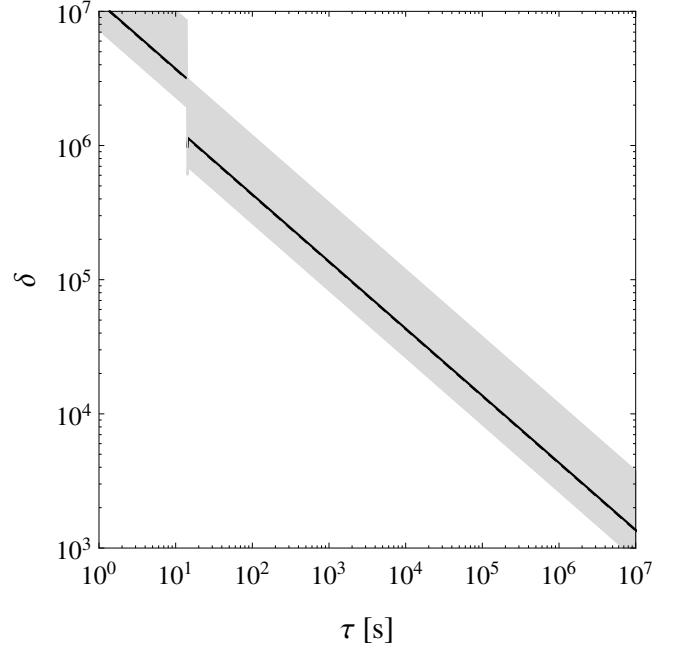


Figure 5: Determination of $\delta(\tau)$ depending only on $m_{\text{hdm}}^{\text{eff}}$ exploiting (21) and (22) with fixed T_{ν_s} . For a fixed $m_{\text{hdm}}^{\text{eff}}$ the later the decay the smaller the mass hierarchy might be. The solid line corresponds to $m_{\text{hdm}}^{\text{eff}}/\text{eV} = 0.41 \pm 0.26$ with its $2\text{-}\sigma$ range as grey band, while $\Delta N_{\text{eff}} = 0.61$ is kept fix. The jump around $t \sim 10 \text{ s}$ corresponds to the time of e^+e^- annihilation. Planck’s CMB only upper bound $m_{\text{hdm}}^{\text{eff}} < 0.59 \text{ eV}$ and $\Delta N_{\text{eff}} < 0.86$ (both 95%) [1] is barely visible right on the solid line. We have chosen $g_{\text{hdm}} = 1$ for the figure. If the decay is into identical particles, the vertical axis should carry x_2^{-1} and all lines shift up by $1/2$ as $g_{\text{hdm}} = 2$.

Late decay – How to mimic a sterile neutrino in N_{eff} is shown in Fig. 3. The horizontal axis spans the full range of considered lifetimes. We take the temperature dependence of g_{*s} fully into account. Around $\tau \sim 10 \text{ s}$, when e^+e^- annihilate away, g_{*s} decreases. The curves stay straight as for the same reason the temperature of the Universe increases, both effects cancelling each other up to the difference between $g_*^0 \simeq 3.384$ and $g_{*s}^0 \simeq 3.938$. It is roughly $(g_{*s}^0/g_*^0)^{1/3} \simeq 1.05$. The time when BBN ends $t_{\text{bbn}}^{\text{end}}$ is highlighted. Decays before this time increase the effective number of neutrino species inferred from BBN $\Delta N_{\text{eff}}|_{\text{bbn}}$ partially as quantified in [39]. Comparing (10) and (21) we see that a higher T_{ν_s} is mimicked by a larger energy density of the mother at decay. This has been shown in [40] solving the corresponding Boltzmann equations numerically. The values chosen for ΔN_{eff} , which are in one-to-one correspondence with T_{ν_s} via (10), are given in the figure caption. We can see how a narrow range of T_{ν_s} maps onto a narrow range of $mY(\tau)$ forming a strip in the $mY\text{-}\tau$ plane.

After having fixed mY/T_{d} we can use Fig. 4, which is obtained by setting (11) equal to (22), to determine the

correct $\delta(mY)$ mimicking the effective HDM mass

$$m_{\text{hdm}}^{\text{eff}} \simeq 26.0 g_{\text{hdm}} \frac{mY}{\delta + 1} \frac{g_{*s}^{\text{d}}}{g_{*s}^{\text{o}}} \quad (26)$$

$$\text{or } \simeq 52.0 x_2 mY \frac{g_{*s}^{\text{d}}}{g_{*s}^{\text{o}}}.$$

Alternatively, we can use (21) to re-write (22), which equals (11), obtaining

$$\delta \simeq 5 \times 10^3 \frac{T_{\text{d}}}{\text{keV}} \Delta N_{\text{eff}} \frac{\text{eV}}{m_{\text{hdm}}^{\text{eff}}} \left(\frac{g_{*s}^{\text{d}}}{g_{*s}^{\text{o}}} \right)^{\frac{4}{3}} \frac{g_{\text{hdm}}}{2} - 1 \quad (27)$$

which allows to provide Fig. 5. For a given lifetime we can thus read off the corresponding mY and δ to mimic any ‘‘observed’’ sterile neutrino parameters.

Altogether, we found the following prescription: i) Determine $mY(\tau)$ using (21) such that the desired ΔN_{eff} is obtained. ii) Determine $\delta(\tau)$ using (27) such that the desired $m_{\text{hdm}}^{\text{eff}}$ is obtained while ΔN_{eff} is kept fixed. This makes dpHDM indistinguishable from ν_s HDM in N_{eff} and $m_{\text{hdm}}^{\text{eff}}$. For illustration, we translate (1) into

$$\frac{mY}{T_{\text{d}}} \left(\frac{g_{*s}^{\text{o}}}{g_{*s}^{\text{d}}} \right)^{\frac{1}{3}} = 0.060 \pm 0.029$$

$$(\text{‘‘1-}\sigma\text{’’}; 0.05 \text{ s} < \tau < 5.2 \times 10^{10} \text{ s}) \quad (28)$$

and

$$x_2 mY \frac{g_{*s}^{\text{d}}}{g_{*s}^{\text{o}}} = (7.9 \pm 2.5) \times 10^{-3} \text{ eV}$$

$$(\text{‘‘1-}\sigma\text{’’}; 0.05 \text{ s} < \tau < 5.2 \times 10^{10} \text{ s}) \quad (29)$$

for a scenario with mass-degenerate daughters. If the daughters possess a large mass hierarchy, such that $g_{\text{hdm}} = 1$, proceed as discussed below (25).

It is important that –in contrast to the early decay case– the assumption of BBN consistency is wrong, because for a late cosmological decay $N_{\text{eff}|_{\text{bbn}}} < N_{\text{eff}|_{\text{cmb}}}$. The possibility of late cosmological decays motivates determinations of $N_{\text{eff}|_{\text{cmb}}}$, where the primordial abundance of light elements is constrained from direct observations only, so *really* independent of cosmology at earlier times, and fixed $N_{\text{eff}|_{\text{bbn}}} = N_{\text{eff}}^{\text{sm}}$. For earlier related work with a different approach in a different scenario see [41].

A degeneracy – For the early decay we can exploit (17), (19) and (23) to obtain the following *parameter degeneracy* relation

$$T_{\text{ed}}^{\text{nr}} = \frac{180\zeta(3)}{7\pi^4} \left(\frac{11}{4} \right)^{\frac{1}{3}} \frac{m_{\text{hdm}}^{\text{eff}}}{\Delta N_{\text{eff}}} \frac{2}{g_{\text{hdm}}}. \quad (30)$$

Analogously, if we use (21) and (22) eliminating mY , we can single out $T_{\text{d}}(\delta + 1)/((\delta + 1)^2 - 1)$. Inserting the resulting expression into (19) we obtain

$$T_{\text{ld}}^{\text{nr}} \simeq 0.445 \frac{m_{\text{hdm}}^{\text{eff}} g_{*s}^{\text{o}}}{\Delta N_{\text{eff}} g_{*s}^{\text{d}} g_{\text{hdm}}} \frac{2}{g_{\text{hdm}}}. \quad (31)$$

We see that the main physical effects are described by only two independent parameters. In other words, there is a degeneracy among the three physical parameters. The same degeneracy has been identified for the thermal relic case in [42].⁵ Indeed, we find exactly the same degeneracy, i.e. the same numerical value, if we consider $g_{\text{hdm}} = 2$ and –for the late decay– $g_{*s}^{\text{d}} = g_{*s}^{\text{o}}$, which is fulfilled after e^+e^- annihilation, so in a large part of the parameter space. Viewed as a constraint equation the degeneracy in physical parameters reduces the number of independent degrees of freedom describing dpHDM from three to two. Considering N_{eff} and $m_{\text{hdm}}^{\text{eff}}$ only, which can describe the main physical effects, an early cosmological particle decay, as well as a decay after e^+e^- annihilation, as origin of HDM is indistinguishable from ν_s HDM, if the daughters are mass degenerate. The mimicry is ‘‘perfect’’ in the sense that there is no new signature in the main physical effects as those contained in ν_s HDM parameters (T_{ν_s} or ΔN_{eff} and m_{ν_s} or $m_{\text{hdm}}^{\text{eff}}$).

More complex scenarios If the daughters do not possess a large mass hierarchy, $m_1 \lesssim m_2$, their impact on observables is similar to the case of two sterile neutrinos with equal temperature but different mass. Moreover, considering two sterile neutrino populations with sufficiently different temperatures, one neutrino might not account for Ω_{hdm} as being still relativistic today and thus forming dark radiation. This situation would correspond to two dark decay modes in the cosmological particle decay, one for dark radiation and one for HDM. All we would like to point out here is that these scenarios are more complex also in the case of a thermal relic. Consequently, they are not discussed in this work and left for future work.

The arguably most interesting case is found if the heavier daughter forms HDM and the lighter one dark radiation. Then the temperature of the universe, when the HDM becomes non-relativistic is a factor of two larger as $g_{\text{hdm}} = 1$ in (30) and (31), respectively. Translated to sterile neutrinos, this situation is represented by two sterile neutrino populations with the same temperature, while one is massive and the other one is massless. Interestingly, current (non-zero) mean values for a HDM contribution correspond to T^{nr} s around T_{γ}^{dpl} , see Fig. 2. If T^{nr} becomes significantly larger than T_{γ}^{dpl} due this factor of two, this effect could be used to distinguish this case, because the impact on the CMB becomes qualitatively different for $T^{\text{nr}} > T_{\gamma}^{\text{dpl}}$ [33]. As mentioned already, the non-observation of such an impact constrains the size of $m_{\text{hdm}}^{\text{eff}}$. While we do not attempt quantitative statements, here, it seems that the increase in $m_{\text{hdm}}^{\text{eff}}$ would be in stronger tension with the CMB data for $g_{\text{hdm}} = 1$. This could disfavour this case compared to the case of mass-

⁵ It has been used to show that a Dodelson-Widrow model shares the same ‘‘observable’’ parameters as a thermal sterile neutrino model with adjusted mass and temperature.

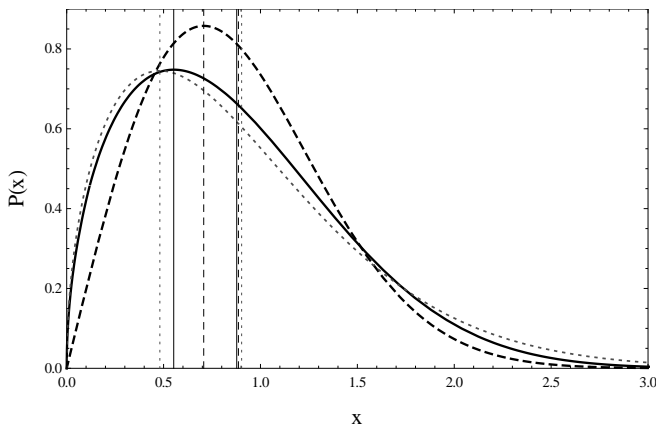


Figure 6: Normalised, time-invariant probability distribution $P(x = p/p(\tau, t))$ for finding a relativistic particle from two-body decay (decaying particle at rest) within the infinitesimal momentum interval $[p, p + \delta p]$. In the early decay case the mother may dominate (black, solid) the Universe. For a late decay the Universe is radiation dominated (black, dashed). The Universe becomes matter-dominated (grey, dotted) at very late times only. Highlighted with corresponding lines are the maxima and means.

degenerate daughters. On the other hand, if a late decay occurs before e^+e^- annihilation, the daughters become non-relativistic at a time $g_{*s}^d/g_{*s}^0 \simeq 2.73$ later which reduces the constraining power from the direct impact on the CMB.

For lower T^{nr} it has been argued in [43] that an optimal LSST-type wide field survey might provide the ability to distinguish between thermal, fermionic HDM (Majorana fermion) and thermal, bosonic HDM (scalar). For fixed Ω_{hdm} the scalar becomes non-relativistic at a temperature, which is a factor of 3/2 larger than in the case of a fermion. This is simply the increase in mass compensating the factor considering the scalar particle nature in (11). We might conclude that the same observations are able to differ between ν_s HDM and dpHDM where the heavier daughter forms HDM and the lighter one dark radiation. However, on the observed non-linear scales N-body simulations appear to become necessary [44] and HDM infall might become an observable effect with the increased precision [43]. The exploration of this interesting opportunity to probe the origin of HDM is beyond the scope of this work. In future work, all discussed scenarios can be implemented in CAMB⁶ or CLASS⁷ easily, because they can be represented by thermal fermion populations as just described and summarised in Tab. I.

⁶ <http://camb.info/>

⁷ <http://class-code.net/>

B. Breakdown in the Third

It is a simplification to reduce the physical impact of any population of massive free-streaming particles to the effects listed in Sec. II. The free-streaming effect must depend on the details of the momentum distribution $f(p)$ of the population. For illustration imagine a distribution with a sharp peak close to $p = 0$. Such particles would act as cold dark matter and thus should not be counted within the massive free-streaming component (11). Furthermore, the average considered in (5) were between cold and hot particles, so that the correct physical effects were not captured.

Observables and statistical moments – Distribution functions can be specified by their moments $Q^{(n)}$. This has been done for the Fermi-Dirac (active neutrino) distribution $f_{\text{fd}}(y) = 1/(e^y + 1)$ with comoving momentum $y = pa$ in [45]. As their result can be adapted to the sterile neutrino case straightforwardly, we sketch decisive steps in Appendix B. For a thermal population of sterile neutrinos we define

$$Q_{\nu_s}^{(n)} = \frac{1}{\pi^2} \left(\frac{4}{11} \right)^{\frac{3+n}{3}} \left(\frac{T_{\nu_s}}{T_\nu} \right)^{3+n} T^{3+n} \int y^{2+n} f_{\text{fd}}(y) dy. \quad (32)$$

The (first two) cosmological parameters can be expressed by these moments as

$$N_{\text{eff}} = 3.046 + \frac{120}{7\pi^2} \left(\frac{11}{4} \right)^{\frac{4}{3}} T^{-4} Q_{\nu_s}^{(1)} \quad (33)$$

and

$$\Omega_{\nu_s}^0 = \frac{m_{\nu_s}}{\rho_c} \left(\frac{T_0}{T} \right)^3 Q_{\nu_s}^{(0)} \Leftrightarrow \Omega_{\nu_s}^0 h^2 \simeq 0.160 \frac{m_{\text{hdm}}^{\text{eff}}}{\text{eV}} \Delta N_{\text{eff}}^{\frac{3}{4}} T^{-3} Q_{\nu_s}^{(0)}. \quad (34)$$

We see that N_{eff} and $\Omega_{\nu_s}^0$ probe the first two moments of the momentum distribution function.

If the mother does not dominate the Universe at her decay, the momentum distribution function of relativistically emitted daughters (cf. appendix of [15] and [35]) as function of comoving momentum y reads

$$df(y) = n_{\text{ini}} c p_{\text{ini}}^{-c} y^{c-1} e^{-(y/p_{\text{ini}})^c} dy, \quad (35)$$

where n_{ini} denotes the number density of daughters at decay and $p_{\text{ini}} = m(1 - (\delta + 1)^{-2})/2$ or $= m(1 - 4x_2^2)^{1/2}/2$ their initial momentum. For the considered lifetime range it is well approximated by $p_{\text{ini}} \simeq m/2$. In Fig. 6 we depicted the corresponding probability distribution function.

For the late decay we use explicitly that the Universe is radiation dominated, so that $c \equiv 3(1 + \omega)/2 = 2$ as the equation of state of the Universe, $p = \omega\rho$, is given by $\omega = 1/3$ in that case. Nevertheless, our treatment could be applied to any expansion law with $c > 0$. By inspection of (35) we can see that the distribution function

decays as e^{-y} for large comoving momenta as the neutrino distribution function considered in [45]. We define the moments as

$$Q_{\text{dec}}^{(n)} = \frac{n_{\text{ini}}}{T_{\text{d}}^3} \left(\frac{p_{\text{ini}}}{T_{\text{d}}} \right)^n \left(\frac{g_{*s}^0}{g_{*s}^{\text{d}}} \right)^{\frac{n}{3}} T^{3+n} \int cy^{c+n-1} e^{-y^c} dy \quad (36)$$

Then the (first two) cosmological parameters expressed by these moments read

$$N_{\text{eff}} = 3.046 + \frac{120}{7\pi^2} \left(\frac{11}{4} \right)^{\frac{4}{3}} T^{-4} Q_{\text{dec}}^{(1)} \quad (37)$$

and

$$\begin{aligned} \Omega_{\text{dec}}^0 &= \frac{g_{\text{hdm}}}{2} \frac{m_2}{\rho_c} \left(\frac{T_0}{T} \right)^3 Q_{\text{dec}}^{(0)} \Leftrightarrow \\ \Omega_{\text{dec}}^0 h^2 &\simeq 0.160 \frac{g_{\text{hdm}}}{2} \frac{m_2}{\text{eV}} T^{-3} Q_{\text{dec}}^{(0)} \end{aligned} \quad (38)$$

Note that $n_{\text{ini}} = 2n$. We identify two dimensionless, independent parameters $n_{\text{ini}}/T_{\text{d}}^3$ and $p_{\text{ini}}/T_{\text{d}}$ in accordance with the previous discussion. In future work, these could be determined with a Markov Chain Monte Carlo likelihood analysis. Our discussion from (32) to (38) is an alternative way to demonstrate why the mimicry in N_{eff} and $m_{\text{hdm}}^{\text{eff}}$ is "perfect".

In the case of a dominating mother, the simple analytic form (35) is invalid. Boltzmann equations need to be solved numerically, cf. [35]. In Fig. 6 we depicted the resulting probability distribution in the limit of strong dominance, $\rho/\rho_{\text{rad}} \gg 1$, at decay. Concerning the moments (36), the factor $g_{*s}^0/g_{*s}^{\text{d}}$ were absent and the integral could not be performed analytically.

Root-mean-square of absolute momenta – The momentum distribution function of a thermal relic differs from the momentum distribution function of relativistic decay products, cp. (B1) and (35). The two available degrees of freedom have been used to achieve perfect mimicry in the first two cosmological parameters, which have been expressed by the first two moments of the distribution functions. Therefore, the *mimicry must break down* if the next (third) cosmological parameter, which is to be expressed by the next higher moment of the distribution function, is taken into account. The number of parameters to be mimicked then exceeds the number of degrees of freedom.

We identify the third cosmological parameter as the root-mean-square of absolute momenta $\langle p \rangle_{\text{rms}}$ –or, equivalently, the root-mean-square of absolute velocities today⁸–, which is given by the quadratic mean of the distribution of absolute momenta. This quadratic mean is equal to the skewness of the momentum distribution

keeping the directional information. In general, the skewness is the next higher moment following the quadratic mean. The next higher moment to the skewness is the kurtosis. Giving preference to dimensionless parameters we define the *normalised root-mean-square of absolute momenta*

$$\gamma_{\text{rms}} \equiv \frac{\langle p \rangle_{\text{rms}}}{\langle p_{\nu} \rangle_{\text{rms}}} \quad (39)$$

where $\langle p_{\nu} \rangle_{\text{rms}}$ is the root-mean-square of the absolute momentum of the active neutrinos (B7), so that $\gamma_{\nu}^{\text{rms}} = 1$ by definition. The root-mean-squares of absolute momenta can be expressed by moments of the corresponding momentum distribution functions. This can be understood by reminding that the number density $n = Q^{(0)}$ and the relativistic energy density $\rho = \langle p \rangle n = Q^{(1)}$, so that the mean absolute momentum $\langle p \rangle = Q^{(1)}/Q^{(0)}$. Analogously, $\langle p \rangle_{\text{rms}} = (Q^{(2)}/Q^{(0)})^{1/2}$.

For a thermal sterile neutrino population we find

$$\langle p_{\nu_s} \rangle_{\text{rms}} = \left(\frac{15\zeta(5)}{\zeta(3)} \right)^{\frac{1}{2}} \left(\frac{4}{11} \right)^{\frac{1}{3}} \frac{T_{\nu_s}}{T_{\nu}} T \simeq 3.6 T_{\nu_s}, \quad (40)$$

which implies with (B7) a normalised root-mean-square of absolute momenta

$$\gamma_{\nu_s}^{\text{rms}} = \frac{T_{\nu_s}}{T_{\nu}} = \Delta N_{\text{eff}}^{\frac{1}{4}} \quad (41)$$

that can be expressed by lower momenta (33). This is to be expected, since $\gamma_{\nu_s}^{\text{rms}}$ cannot carry additional information as both neutrino species possess a Fermi-Dirac distribution.

The momentum distribution function of the sterile neutrinos in the popular Dodelson-Widrow (DW) scenario [46] (a.k.a. "non-resonant production scenario") reads

$$f_{\text{dw}}(y) = \frac{\chi}{e^y + 1} = \chi f_{\text{fd}}. \quad (42)$$

The sterile neutrinos share the same "observable" parameters (ΔN_{eff} , Ω_{hdm}^0 , T^{nr}) as a thermal population with $m_{\nu_s}^{\text{th}} = \chi^{1/4} m_{\nu_s}^{\text{dw}}$ and $T_{\nu_s}^{\text{th}} = \chi^{1/4} T_{\nu}$. For these two models it has been shown by a change of variable in the background and linear perturbation equations that the two models are strictly equivalent for cosmological observables [47]. We confirm this result with the expansion of the distribution functions in moments. Compensating the scaling factor χ , the two models share the same (Fermi-Dirac) distribution function. Higher moments can be expressed by lower ones and the distribution functions are identical. Therefore, they are indistinguishable for cosmological observations even if higher moments are taken into account. In other words, their *mimicry is perfect to arbitrary order in moments*.

This is *qualitatively different for the decay products* of a cosmological particle decay mimicking a thermal sterile neutrino population. For daughters emitted in a late

⁸ If clustering can be neglected, today's root-mean-square of absolute velocities $\langle v^0 \rangle_{\text{rms}} = \langle p^0 \rangle_{\text{rms}}/m$.

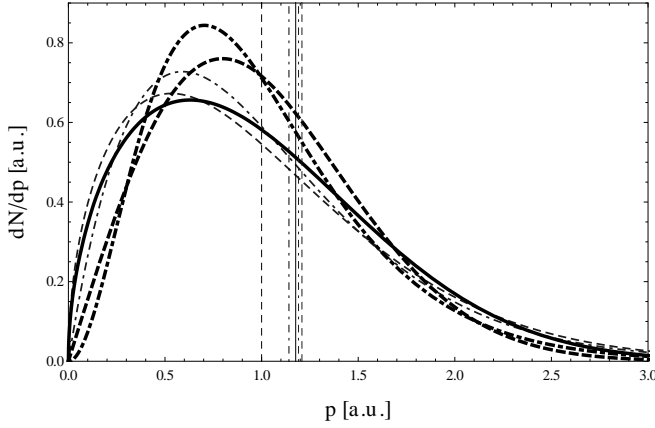


Figure 7: Momentum distribution functions with perfect mimicry in the first two cosmological observables corresponding to their first two moments and their next higher moment. Depicted are distributions for the early decay (black, solid), the late decay (black, dashed), Pauli-Dirac (black, dash-dotted), Einstein-Bose (grey, dash-dotted) and decay in a matter-dominated universe (grey, dashed). Zeroth and first moment have been set to unity. Vertical lines mark the corresponding second moments (= skewness). Units are arbitrary.

decay we find

$$\langle p_{\text{dec}} \rangle_{\text{rms}} = \left(\frac{Q_{\text{dec}}^{(2)}}{Q_{\text{dec}}^{(0)}} \right)^{\frac{1}{2}} = \frac{p_{\text{ini}}}{T_{\text{d}}} T \left(\frac{g_{*s}^0}{g_{*s}^{\text{d}}} \right)^{\frac{1}{3}}, \quad (43)$$

where we used that $\int cy^{c+n-1}e^{-y^c}dy = 1$ for $c = 2$ in both cases, $n = 0$ and $n = 2$. We obtain a very simple, exact expression. With (B7) this implies

$$\begin{aligned} \gamma_{\text{ld}}^{\text{rms}} &= \left(\frac{\zeta(3)}{15\zeta(5)} \right)^{\frac{1}{2}} \left(\frac{11}{4} \right)^{\frac{1}{3}} \left(\frac{g_{*s}^0}{g_{*s}^{\text{d}}} \right)^{\frac{1}{3}} \frac{p_{\text{ini}}}{T_{\text{d}}} \\ &\simeq 0.389 \frac{p_{\text{ini}}}{T_{\text{d}}} \left(\frac{g_{*s}^0}{g_{*s}^{\text{d}}} \right)^{\frac{1}{3}}, \end{aligned} \quad (44)$$

which can be expressed as

$$\gamma_{\text{ld}}^{\text{rms}} \simeq 0.0105 \frac{\Delta N_{\text{eff}} g_{\text{hdm}}}{\Omega_{\text{ld}}^0 h^2 2} \quad (45)$$

by lower moments. Again, this must be, since there are no further parameters. All higher momenta are fixed by the first two.

The predicted deviation between ν_s HDM and dpHDM (with $g_{\text{hdm}} = 2$) in the normalised root-mean-squares of absolute momenta is thus found by combining (45) and (41) as

$$\gamma_{\text{ld}}^{\text{rms}}/\gamma_{\nu_s}^{\text{rms}} \simeq 0.0105 \frac{\Delta N_{\text{eff}}^{\frac{3}{4}}}{\Omega_{\text{dec}}^0 h^2} \simeq 0.989 \frac{\Delta N_{\text{eff}}^{\frac{3}{4}}}{m_{\text{hdm}}^{\text{eff}}/\text{eV}}. \quad (46)$$

Under the crude assumption of Gaussian error propagation this implies for (1) a prediction,

$$\gamma_{\text{ld}}^{\text{rms}}/\gamma_{\nu_s}^{\text{rms}} = 1.66 \pm 0.81 (1-\sigma). \quad (47)$$

daughter masses	mimicry in 1st two	opportunity?	ν_s equivalent
$m_1 \ll m_2$	✓	$2 \times$ larger T^{nr}	$2\nu_s: T_1 = T_2,$ $m_2 > m_1 = 0$
$m_1 = m_2$	✓	breaks down in $\langle p \rangle_{\text{rms}}$	”perfect” for current obs.
$m_1 \lesssim m_2$	✓	as ν_s equivalent	$2\nu_s: T_1 = T_2,$ $m_2 \gtrsim m_1 > 0$

Table I: Overview of different cases depending on the daughter masses. In every case there is mimicry in the first two cosmological observables. Given are opportunities to distinguish these cases from ν_s HDM and how they are represented by thermal ν_s populations.

Since the momentum distribution functions differ between early and late decay as can be seen in Fig. 7, these numbers differ between these two cases. We find $\langle p_{\text{ed}} \rangle_{\text{rms}} \simeq 1.03 \times \langle p_{\text{ld}} \rangle_{\text{rms}}$ and thus

$$\gamma_{\text{ed}}^{\text{rms}}/\gamma_{\nu_s}^{\text{rms}} = 1.72 \pm 0.84 (1-\sigma). \quad (48)$$

So there is a 66% (72%) difference in the mean for the late (early) decay but the uncertainty of the prediction is decisively larger. Obviously, the difference to ν_s HDM is too small to be detected in an extended analysis that would have to try to determine γ^{rms} as additional free parameter. Not to mention that the observations need to be sensitive to this effect. We do not expect that current observations or observations in the near future will be able to distinguish dpHDM from ν_s HDM in all cases. In this sense, the mimicry can be ”perfect for our limited observational capabilities.”⁹

It is tempting to look for a first hint if this negative conclusion could change in the next decade. With full Planck data available the galaxy survey EUCLID (to be launched 2020) will increase sensitivities dramatically by roughly an order of magnitude, cf. [48]. Including galaxy surveys, eBOSS and DESI, and a new (Stage-IV) CMB polarimeter, expected sensitivities go down to $\sigma(\sum m_\nu) = 16$ meV and $\sigma(N_{\text{eff}}) = 0.020$ [49]. These sensitivities would imply 1- σ errors in the prediction of $\gamma_{\text{dec}}^{\text{rms}}/\gamma_{\nu_s}^{\text{rms}}$ that are nine times smaller than the predicted deviation for the current mean values (1). However, these means can and will change, but for means half the size the 1- σ errors were still 3.5 times smaller than the predicted deviation. If not from testing our standard interpretation alone, the opportunity to distinguish ν_s HDM from dpHDM, motivates to study which future observations can how far probe the root-mean-square of absolute momenta of a free-streaming population.

⁹ This usage of the notion of mimicry is actually closest to mimicry in biology.

IV. SUMMARY AND CONCLUSIONS

As summarised in Tab. I, it depends on the daughter masses where and how the mimicry breaks down. Every case can be implemented easily as ν_s populations in existing numerical tools. If the daughters do possess a large mass hierarchy, the temperature when dpHDM becomes non-relativistic is larger by a factor of two compared to ν_s HDM, so that this case might be in stronger tension with CMB data. If the daughters are mass degenerate, they are indistinguishable from ν_s HDM in analyses like [3].

Connecting cosmological "observables" with moments of the momentum distribution functions depicted in Fig. 7, we find that for mass-degenerate daughters the mimicry breaks down only, if the next higher moment of the momentum distribution, the skewness, is considered. We define the *normalised root-mean-square of absolute momenta* and find sizeable differences in its predicted value between dpHDM and ν_s HDM. While these are certainly too small for current observations, this is a *qualitative difference* compared to the attempt to distinguish different ν_s HDM models, where the mimicry is perfect to arbitrary order of moments.

Other opportunities depend on the time of decay: For certain times during the BBN era, dpHDM becomes non-relativistic later than ν_s HDM. A decay after BBN increases $N_{\text{eff}}|_{\text{cmb}} > N_{\text{eff}}|_{\text{bbn}} = N_{\text{eff}}^{\text{sm}}$, which motivates analyses that drop the BBN consistency relation.

To conclude, current cosmological observations are sensitive to sub-eV, not fully-thermalised HDM characterised by $\Delta N_{\text{eff}} < 1$ and $m_{\text{hdm}}^{\text{eff}} < \text{eV}$. In that case, from a cosmological point of view ν_s HDM is not preferred over dpHDM, neither from theoretical nor practical simplicity. Our (current) blindness for the case of mass-degenerate daughters, should prevent us from premature conclusions when interpreting signals like (1). Fortunately, there are various cases that can be considered easily and gainfully in likelihood analyses utilising available data already. After our proof of principle that, in contrast to different, thermal ν_s HDM models, the mimicry of dpHDM breaks down at least in the root-mean-square of absolute momenta, it is an open question which observation due to which effect will be able to distinguish the two possibilities.

Acknowledgements

I would like to thank Jan Hamann for valuable discussions. I acknowledge support from the German Academy of Science through the Leopoldina Fellowship Programme grant LPDS 2012-14.

Appendix A: Free-streaming scale and transition time

Starting from (93) in [25],

$$k^{\text{fs}}(T) = \left(\frac{3}{2} \frac{H^2(T) a^2(T)}{\langle v \rangle(T)} \right)^2, \quad \lambda^{\text{fs}}(T) = 2\pi \frac{a(T)}{k^{\text{fs}}(T)}, \quad (\text{A1})$$

we approximate the average absolute velocity of the population $\langle v \rangle = \langle p \rangle / m$ at the transition, $\langle p \rangle = m$, as the speed of light c . We assume that it then decreases as $a^{-1} \propto T$, so that $\langle v \rangle(T) = cT/T^{\text{nr}}$, if T^{nr} denotes the temperature of the Universe at the transition.¹⁰ The scale factor can be expressed in temperatures as $a(T)/a_0 = T_0/T$ and $H^2 = H_0^2 (\Omega_{\text{m}}(T/T_0)^3 + \Omega_{\Lambda})$. Inserting yields

$$k^{\text{fs}}(T) \simeq 4.08 \times 10^{-4} \left(\Omega_{\text{m}} \left(\frac{T}{T_0} \right)^3 + \Omega_{\Lambda} \right)^{\frac{1}{2}} \frac{T_0 T^{\text{nr}}}{T^2} \frac{h}{\text{Mpc}} \quad (\text{A2})$$

and

$$\lambda^{\text{fs}}(T) \simeq 1.54 \times 10^4 \left(\Omega_{\text{m}} \left(\frac{T}{T_0} \right)^3 + \Omega_{\Lambda} \right)^{-\frac{1}{2}} \frac{T}{T^{\text{nr}}} \frac{\text{Mpc}}{h}. \quad (\text{A3})$$

For $k^{\text{nr}} = k^{\text{fs}}(T^{\text{nr}})$ we obtain (4). For reference we provide the often used free-streaming scale of the population today,

$$\lambda^{\text{fs}} \simeq 1.54 \times 10^4 \frac{T_0}{T^{\text{nr}}} h^{-1} \text{Mpc}. \quad (\text{A4})$$

Consistently we see from (93) of [25]

$$\lambda^{\text{fs}}(t^{\text{nr}}) = 2\pi(2/3)^{1/2} \langle v(t^{\text{nr}}) \rangle / H(t^{\text{nr}}) = \sqrt{6}\pi t^{\text{nr}}, \quad (\text{A5})$$

where we used $\langle v(t^{\text{nr}}) \rangle = 1$ and $H = 2/(3t)$ in matter domination. We calculate the time when a population becomes non-relativistic in a Universe filled with radiation and matter as $t^{\text{nr}} = \frac{t_{\text{eq}}}{2-\sqrt{2}} \left(\left(\frac{T_{\text{eq}}}{T^{\text{nr}}} - 2 \right) \left(\frac{T_{\text{eq}}}{T^{\text{nr}}} + 1 \right)^{1/2} + 2 \right)$, where $T_{\text{eq}}(t_{\text{eq}})$ denotes the temperature (time) at matter-radiation equality.

Appendix B: Neutrino distribution specified by its moments

This appendix shall improve the accessibility of Sec. III B for the reader. We repeat findings of Cuoco, Lesgourgues, Mangano and Pastor in [45] and refer the reader to the original work.

¹⁰ As a side note, we could also calculate $\langle v \rangle = \langle E_{\text{kin}} \rangle / m = \rho_{\text{kin}} / (mn)$ and insert appropriate expressions for the kinetic energy density ρ_{kin} .

The solution to the collisionless kinetic equations in a Lemaitre-Friedman-Robertson-Walker universe is a Fermi-Dirac function $f(\vec{p}) = 1/(e^{(E-\mu)/T} + 1)$ with particle energy $E^2 = |\vec{p}|^2 + m^2 = p^2 + m^2$. We are interested in the standard situation with vanishing chemical potential μ and early times, when neutrinos are ultra-relativistic. Considering a radiation dominated universe, where $T \propto a^{-1}$, and defining the comoving momentum $y = pa$ one finds

$$df(p, T_\nu) = \frac{1}{\pi^2} T_\nu^3 \frac{y^2}{e^y + 1} dy, \quad (\text{B1})$$

where isotropy has been exploited to reduce the dimension of the differential and which is normalised such that the integral yields the number density as required. One can define a set of moments

$$Q_\nu^{(n)} = \frac{1}{\pi^2} \left(\frac{4}{11}\right)^{\frac{3+n}{3}} T_\nu^{3+n} \int y^{2+n} f(y) dy \quad (\text{B2})$$

in terms of the neutrino temperature $T_\nu = (4/11)^{1/3} T$. These moments can specify the neutrino distribution $df(y)$ regardless of the specific case at hand. In [45] this is used to explore observation prospects for non-thermal contributions to the standard neutrino spectrum. If the distribution decays at large comoving momentum as e^{-y} , it admits moments of all orders. In [45] the neutrino distribution is given in terms of its moments as

$$df(y) = \frac{y^2}{e^y + 1} \sum_{m=0}^{\infty} \sum_{k=0}^m c_k^{(m)} Q_\nu^{(k)} T_\nu^{-k} P_m(y) dy \quad (\text{B3})$$

with $P_m(y) = \sum_{k=0}^m c_k^{(m)} y^k$, m being the degree of $P_m(y)$ and $c_k^{(m)}$ being a coefficient, denoting the set of polynomials orthonormal with respect to the measure $y^2/(e^y + 1)$, i.e., $\int_0^\infty dy \frac{y^2}{e^y + 1} P_n(y) P_m(y) = \delta_{nm}$. For a Fermi-Dirac

distribution all moments can be expressed in terms of the lowest moment $Q_\nu^{(0)} = n_\nu$ or, equivalently, as functions of the temperature T_ν since it is the only independent parameter. For neutrinos the (first two) cosmological observables can be written as

$$N_{\text{eff}} = \frac{120}{7\pi^2} T_\nu^{-4} \sum_\alpha Q_{\nu\alpha}^{(1)} \quad (\text{B4})$$

and

$$\begin{aligned} \Omega_\nu^0 &= \frac{\sum m_\nu}{\rho_c} Q_\nu^{(0)} \left(\frac{T_0}{T}\right)^3 \\ &\Leftrightarrow \Omega_\nu^0 h^2 \simeq 0.162 \frac{\sum m_\nu}{\text{eV}} T^{-3} Q_\nu^{(0)}, \end{aligned} \quad (\text{B5})$$

where it is assumed that the three neutrinos share the same distribution today and the small correction from e^+e^- annihilation, $N_{\text{eff}}^{\text{sm}} = 3.046 \neq 3$, is incorporated in the numerical prefactor. In [45] N_{eff} and f_ν are used to probe deviations from the standard neutrino spectrum in the first two moments.

Also the following facts are used in our discussion: The average absolute neutrino momentum $\langle p_\nu \rangle$ expressed by moments of their distribution (B2) reads

$$\langle p_\nu \rangle = \frac{Q_\nu^{(1)}}{Q_\nu^{(0)}} = \frac{7\pi^4}{180\zeta(3)} \left(\frac{4}{11}\right)^{\frac{1}{3}} T \simeq 3.15 T_\nu \quad (\text{B6})$$

and the root-mean-square of absolute momenta $\langle p_\nu \rangle_{\text{rms}} = (Q_\nu^{(2)}/Q_\nu^{(0)})^{1/2}$ can be calculated analogously as

$$\langle p_\nu \rangle_{\text{rms}} = \left(\frac{15\zeta(5)}{\zeta(3)}\right)^{\frac{1}{2}} \left(\frac{4}{11}\right)^{\frac{1}{3}} T \simeq 3.6 T_\nu. \quad (\text{B7})$$

-
- [1] Planck Collaboration, P. Ade *et al.*, “Planck 2013 results. XVI. Cosmological parameters”, [arXiv:1303.5076](#) [[astro-ph.CO](#)].
- [2] M. Wyman, D. H. Rudd, R. A. Vanderveld, and W. Hu, “ $\nu\Lambda$ CDM: Neutrinos help reconcile Planck with the Local Universe”, *Phys.Rev.Lett.* **112** (2014) 051302, [arXiv:1307.7715](#) [[astro-ph.CO](#)].
- [3] J. Hamann and J. Hasenkamp, “A new life for sterile neutrinos: resolving inconsistencies using hot dark matter”, *JCAP* **1310** (2013) 044, [arXiv:1308.3255](#) [[astro-ph.CO](#)].
- [4] R. A. Battye and A. Moss, “Evidence for massive neutrinos from CMB and lensing observations”, *Phys.Rev.Lett.* **112** (2014) 051303, [arXiv:1308.5870](#) [[astro-ph.CO](#)].
- [5] M. Costanzi, F. Villaescusa-Navarro, M. Viel, J.-Q. Xia, S. Borgani, *et al.*, “Cosmology with massive neutrinos III: the halo mass function and application to galaxy clusters”, *JCAP* **1312** (2013) 012, [arXiv:1311.1514](#) [[astro-ph.CO](#)].
- [6] G. Efstathiou, “H0 Revisited”, [arXiv:1311.3461](#) [[astro-ph.CO](#)].
- [7] A. Paranjape, “Cosmology with Galaxy Clusters: Systematic Effects in the Halo Mass Function”, [arXiv:1403.3402](#) [[astro-ph.CO](#)].
- [8] B. Leistedt, H. V. Peiris, and L. Verde, “No new cosmological concordance with massive sterile neutrinos”, [arXiv:1404.5950](#) [[astro-ph.CO](#)].
- [9] G. Steigman, “Equivalent Neutrinos, Light WIMPs, and the Chimera of Dark Radiation”, *Phys.Rev.* **D87** (2013) no. 10, 103517, [arXiv:1303.0049](#) [[astro-ph.CO](#)].
- [10] S. Hannestad, R. S. Hansen, and T. Tram, “How secret interactions can reconcile sterile neutrinos with cosmology”, *Phys.Rev.Lett.* **112** (2014) 031802, [arXiv:1310.5926](#) [[astro-ph.CO](#)].
- [11] B. Dasgupta and J. Kopp, “A ménage à trois of eV-scale sterile neutrinos, cosmology, and structure formation”, *Phys.Rev.Lett.* **112** (2014) 031803,

- [arXiv:1310.6337 \[hep-ph\]](#).
- [12] T. Bringmann, J. Hasenkamp, and J. Kersten, “Tight bonds between sterile neutrinos and dark matter”, [arXiv:1312.4947 \[hep-ph\]](#).
- [13] J. Hasenkamp and J. Kersten, “Dark and visible matter with broken R-parity and the axion multiplet”, *Phys.Lett.* **B701** (2011) 660–666, [arXiv:1103.6193 \[hep-ph\]](#).
- [14] J. Hasenkamp, “Dark radiation from the axino solution of the gravitino problem”, *Phys. Lett.* **B707** (2012) 121–128, [arXiv:1107.4319 \[hep-ph\]](#).
- [15] J. Hasenkamp and J. Kersten, “Dark radiation from particle decay: cosmological constraints and opportunities”, *JCAP* **1308** (2013) 024, [arXiv:1212.4160 \[hep-ph\]](#).
- [16] K. J. Bae, H. Baer, and A. Lessa, “Dark Radiation Constraints on Mixed Axion/Neutralino Dark Matter”, *JCAP* **1304** (2013) 041, [arXiv:1301.7428 \[hep-ph\]](#).
- [17] P. Graf and F. D. Steffen, “Dark radiation and dark matter in supersymmetric axion models with high reheating temperature”, *JCAP* **1312** (2013) 047, [arXiv:1302.2143 \[hep-ph\]](#).
- [18] T. Higaki, K. S. Jeong, and F. Takahashi, “A Parallel World in the Dark”, *JCAP* **1308** (2013) 031, [arXiv:1302.2516 \[hep-ph\]](#).
- [19] P. Di Bari, S. F. King, and A. Merle, “Dark Radiation or Warm Dark Matter from long lived particle decays in the light of Planck”, *Phys.Lett.* **B724** (2013) 77–83, [arXiv:1303.6267 \[hep-ph\]](#).
- [20] J. P. Conlon and M. C. D. Marsh, “The Cosmophenomenology of Axionic Dark Radiation”, *JHEP* **1310** (2013) 214, [arXiv:1304.1804 \[hep-ph\]](#).
- [21] J.-C. Park and S. C. Park, “A testable scenario of WIMPZILLA with Dark Radiation”, *Phys.Lett.* **B728** (2014) 41–44, [arXiv:1305.5013 \[hep-ph\]](#).
- [22] D. Hooper, “Is the CMB telling us that dark matter is weaker than weakly interacting?”, *Phys.Rev.* **D88** (2013) 083519, [arXiv:1307.0826 \[hep-ph\]](#).
- [23] C. Kelso, C. A. de S. Pires, S. Profumo, F. S. Queiroz, and P. S. Rodrigues da Silva, “A 331 WIMPY Dark Radiation Model”, *Eur.Phys.J.* **C74** (2014) 2797, [arXiv:1308.6630 \[hep-ph\]](#).
- [24] K. S. Jeong, M. Kawasaki, and F. Takahashi, “Axions as Hot and Cold Dark Matter”, *JCAP* **1402** (2014) 046, [arXiv:1310.1774 \[hep-ph\]](#).
- [25] J. Lesgourgues and S. Pastor, “Massive neutrinos and cosmology”, *Phys.Rept.* **429** (2006) 307–379, [arXiv:astro-ph/0603494 \[astro-ph\]](#).
- [26] G. Mangano *et al.*, “Relic neutrino decoupling including flavour oscillations”, *Nucl. Phys.* **B729** (2005) 221–234, [arXiv:hep-ph/0506164](#).
- [27] C. Giunti, M. Laveder, Y. Li, and H. Long, “Pragmatic View of Short-Baseline Neutrino Oscillations”, *Phys.Rev.* **D88** (2013) 073008, [arXiv:1308.5288 \[hep-ph\]](#).
- [28] J. Kopp, P. A. N. Machado, M. Maltoni, and T. Schwetz, “Sterile Neutrino Oscillations: The Global Picture”, *JHEP* **1305** (2013) 050, [arXiv:1303.3011 \[hep-ph\]](#).
- [29] BICEP2 Collaboration, P. Ade *et al.*, “BICEP2 I: Detection Of B-mode Polarization at Degree Angular Scales”, [arXiv:1403.3985 \[astro-ph.CO\]](#).
- [30] Z. Hou, C. Reichardt, K. Story, B. Follin, R. Keisler, *et al.*, “Constraints on Cosmology from the Cosmic Microwave Background Power Spectrum of the 2500-square degree SPT-SZ Survey”, *Astrophys.J.* **782** (2014) 74, [arXiv:1212.6267 \[astro-ph.CO\]](#).
- [31] Z. Hou, R. Keisler, L. Knox, M. Millea, and C. Reichardt, “How Massless Neutrinos Affect the Cosmic Microwave Background Damping Tail”, *Phys.Rev.* **D87** (2013) 083008, [arXiv:1104.2333 \[astro-ph.CO\]](#).
- [32] R. Burenin, “Possible indication for non-zero neutrino mass and additional neutrino species from cosmological observations”, *Astron.Lett.* **39** (2013) 357–366, [arXiv:1301.4791 \[astro-ph.CO\]](#).
- [33] S. Dodelson, E. Gates, and A. Stebbins, “Cold + hot dark matter and the cosmic microwave background”, *Astrophys.J.* **467** (1996) 10–18, [arXiv:astro-ph/9509147 \[astro-ph\]](#).
- [34] W. Fischler and J. Meyers, “Dark Radiation Emerging After Big Bang Nucleosynthesis?”, *Phys.Rev.* **D83** (2011) 063520, [arXiv:1011.3501 \[astro-ph.CO\]](#).
- [35] R. J. Scherrer and M. S. Turner, “Primordial Nucleosynthesis with Decaying Particles. II. Inert Decays”, *Astrophys. J.* **331** (1988) 33–37.
- [36] J. Hasenkamp and J. Kersten, “Leptogenesis, Gravitino Dark Matter and Entropy Production”, *Phys.Rev.* **D82** (2010) 115029, [arXiv:1008.1740 \[hep-ph\]](#).
- [37] R. Durrer and J. Hasenkamp, “Testing Superstring Theories with Gravitational Waves”, *Phys.Rev.* **D84** (2011) 064027, [arXiv:1105.5283 \[gr-qc\]](#).
- [38] J. M. Cline and P. Scott, “Dark Matter CMB Constraints and Likelihoods for Poor Particle Physicists”, *JCAP* **1303** (2013) 044, [arXiv:1301.5908 \[astro-ph.CO\]](#).
- [39] J. L. Menastrina and R. J. Scherrer, “Dark Radiation from Particle Decays during Big Bang Nucleosynthesis”, *Phys.Rev.* **D85** (2012) 047301, [arXiv:1111.0605 \[astro-ph.CO\]](#).
- [40] D. Hooper, F. S. Queiroz, and N. Y. Gnedin, “Nonthermal dark matter mimicking an additional neutrino species in the early universe”, *Phys.Rev.* **D85** (2012) 063513, [arXiv:1111.6599 \[astro-ph.CO\]](#).
- [41] M. Gonzalez-Garcia, V. Niro, and J. Salvado, “Dark Radiation and Decaying Matter”, *JHEP* **1304** (2013) 052, [arXiv:1212.1472 \[hep-ph\]](#).
- [42] M. A. Acero and J. Lesgourgues, “Cosmological constraints on a light non-thermal sterile neutrino”, *Phys.Rev.* **D79** (2009) 045026, [arXiv:0812.2249 \[astro-ph\]](#).
- [43] S. Hannestad, A. Ringwald, H. Tu, and Y. Y. Wong, “Is it possible to tell the difference between fermionic and bosonic hot dark matter?”, *JCAP* **0509** (2005) 014, [arXiv:astro-ph/0507544 \[astro-ph\]](#).
- [44] S. Bird, M. Viel, and M. G. Haehnelt, “Massive Neutrinos and the Non-linear Matter Power Spectrum”, *Mon.Not.Roy.Astron.Soc.* **420** (2012) 2551–2561, [arXiv:1109.4416 \[astro-ph.CO\]](#).
- [45] A. Cuoco, J. Lesgourgues, G. Mangano, and S. Pastor, “Do observations prove that cosmological neutrinos are thermally distributed?”, *Phys.Rev.* **D71** (2005) 123501, [arXiv:astro-ph/0502465 \[astro-ph\]](#).
- [46] S. Dodelson and L. M. Widrow, “Sterile-neutrinos as dark matter”, *Phys.Rev.Lett.* **72** (1994) 17–20, [arXiv:hep-ph/9303287 \[hep-ph\]](#).
- [47] S. Colombi, S. Dodelson, and L. M. Widrow, “Large scale structure tests of warm dark matter”, *Astrophys.J.*

- [458](#) (1996) 1, [arXiv:astro-ph/9505029](#) [[astro-ph](#)].
- [48] J. Hamann, S. Hannestad, and Y. Y. Wong, “Measuring neutrino masses with a future galaxy survey”, *JCAP* **1211** (2012) 052, [arXiv:1209.1043](#) [[astro-ph.CO](#)].
- [49] K. Abazajian, K. Arnold, J. Austermann, B. Benson, C. Bischoff, *et al.*, “Neutrino Physics from the Cosmic Microwave Background and Large Scale Structure”, [arXiv:1309.5383](#) [[astro-ph.CO](#)].